Science AAAS

Rapid Reductions in North Atlantic Deep Water During the Peak of the Last Interglacial Period

Eirik Vinje Galaasen *et al.*

Science **343**, 1129 (2014);
DOI: 10.1126/science.1248667

References and Notes

1. C. R. Dean *et al.*, *Nat. Nanotechnol.* **5**, 722–726 (2010).
2. K. S. Novoselov *et al.*, *Proc. Natl. Acad. Sci. U.S.A.* **102**, 10451–10453 (2005).
3. A. K. Geim, I. V. Grigorieva, *Nature* **499**, 419–425 (2013).
4. T. Kimura, Y. Tokura, *Annu. Rev. Mater. Sci.* **30**, 451–474 (2000).
5. K. F. Mak, C. Lee, J. Hone, J. Shan, T. F. Heinz, *Phys. Rev. Lett.* **105**, 136805 (2010).
6. A. Splendiani *et al.*, *Nano Lett.* **10**, 1271–1275 (2010).
7. X. Qi, S. Zhang, *Rev. Mod. Phys.* **83**, 1057–1110 (2011).
8. L. Britnell *et al.*, *Science* **340**, 1311–1314 (2013).
9. S. Z. Butler *et al.*, *ACS Nano* **7**, 2898–2926 (2013).
10. L. Novotny, B. Hecht, *Principles of Nano-Optics* (Cambridge Univ. Press, Cambridge, 2006).
11. J. Renger, S. Grafström, L. M. Eng, R. Hillenbrand, *Phys. Rev. B* **71**, 075410 (2005).
12. S. Shen, A. Narayanaswamy, G. Chen, *Nano Lett.* **9**, 2909–2913 (2009).
13. T. Feurer, J. C. Vaughan, K. A. Nelson, *Science* **299**, 374–377 (2003).
14. Y. De Wilde *et al.*, *Nature* **444**, 740–743 (2006).
15. A. Huber, N. Ocelic, D. Kazantsev, R. Hillenbrand, *Appl. Phys. Lett.* **87**, 081103 (2005).
16. T. Taubner, D. Korobkin, Y. Urzhumov, G. Shvets, R. Hillenbrand, *Science* **313**, 1595 (2006).
17. G. Shvets, *Phys. Rev. B* **67**, 035109 (2003).
18. J. A. Schuller, R. Zia, T. Taubner, M. L. Brongersma, *Phys. Rev. Lett.* **99**, 107401 (2007).
19. Materials and methods are available as supplementary materials on *Science* Online.
20. J. Chen *et al.*, *Nature* **487**, 77–81 (2012).
21. Z. Fei *et al.*, *Nature* **487**, 82–85 (2012).
22. F. Keilmann, S. Amarie, *J. Infrared Millimeter Terahertz Waves* **33**, 479–484 (2012).
23. J. M. Atkin, S. Berweger, A. C. Jones, M. B. Raschke, *Adv. Phys.* **61**, 745–842 (2012).
24. Z. Fei *et al.*, *Nano Lett.* **11**, 4701–4705 (2011).
25. R. Hillenbrand, T. Taubner, F. Keilmann, *Nature* **418**, 159–162 (2002).
26. R. Geick, C. H. Perry, G. Rupprecht, *Phys. Rev.* **146**, 543–547 (1966).
27. X. G. Xu, A. E. Tanur, G. C. Walker, *J. Phys. Chem. A* **117**, 3348–3354 (2013).
28. L. M. Zhang *et al.*, *Phys. Rev. B* **85**, 075419 (2012).
29. A. Poddubny, I. Iorsh, P. Belov, Y. Kivshar, *Nat. Photonics* **7**, 948–957 (2013).
30. R. Stanley, *Nat. Photonics* **6**, 409–411 (2012).

Acknowledgments: Work at UCSD was supported by U.S. Department of Energy–Office of Basic Energy Sciences (DOE-BES). The development of nano-FTIR at UCSD is supported by Office of Naval Research (ONR), DOE, Air Force Office of Scientific Research (AFOSR), and NSF. M.M.F. is supported by ONR. P.J.-H. acknowledges support from AFOSR grant number FA9550-11-1-0225. A.S.R. acknowledges DOE grant DE-FG02-08ER46512 and ONR grant MURI N00014-09-1-1063. M.T. and G.D. are supported by NASA. A.H.C.N. acknowledges a National Research Foundation–Competitive Research Programme award (R-144-000-295-281). A.Z., W.G., and W.R. acknowledge support from the Director, Office of Energy Research, BES, Materials Sciences and Engineering Division, of the U.S. DOE under contract no. DE-AC02- 05CH11231, which provided for preparation and characterization of the BN, and from the ONR, which provided for substrate transfer technique. F.K. is a cofounder of Neaspec, producer of the s-SNOM apparatus used in this study.

Supplementary Materials
www.sciencemag.org/content/343/6175/1125/suppl/DC1
Materials and Methods
Supplementary Text
Figs. S1 to S5
References (*31–42*)

4 October 2013; accepted 6 February 2014
10.1126/science.1246833

Rapid Reductions in North Atlantic Deep Water During the Peak of the Last Interglacial Period

Eirik Vinje Galaasen,[1]* Ulysses S. Ninnemann,[1,2] Nil Irvalı,[2] Helga (Kikki) F. Kleiven,[1,2] Yair Rosenthal,[3] Catherine Kissel,[4] David A. Hodell[5]

Deep ocean circulation has been considered relatively stable during interglacial periods, yet little is known about its behavior on submillennial time scales. Using a subcentennially resolved epibenthic foraminiferal $\delta^{13}C$ record, we show that the influence of North Atlantic Deep Water (NADW) was strong at the onset of the last interglacial period and was then interrupted by several prominent centennial-scale reductions. These NADW transients occurred during periods of increased ice rafting and southward expansions of polar water influence, suggesting that a buoyancy threshold for convective instability was triggered by freshwater and circum-Arctic cryosphere changes. The deep Atlantic chemical changes were similar in magnitude to those associated with glaciations, implying that the canonical view of a relatively stable interglacial circulation may not hold for conditions warmer and fresher than at present.

Future climate could be affected on a global scale if the circulation of North Atlantic Deep Water (NADW), the main water mass ventilating the deep Atlantic (Fig. 1) (*1*), is altered. Such changes could have widespread and long-lasting impacts—including, for example, on regional sea level (*2*), the intensity and pacing of Sahel droughts (*3*), and the pattern and rate of ocean acidification and CO_2 sequestration (*4*). However, the response of NADW to high-latitude warming and ocean freshening, both of which would decrease source region density and potentially inhibit NADW formation, remains a key uncertainty in future climate projections. Model estimates range from nearly no change to ~50% reduction in Atlantic Meridional Overturning Circulation by 2100 CE (*5*). Compounding the uncertainty, models may inherently underestimate the possibility for abrupt and large changes (*6*), and there may even be critical stability thresholds in surface ocean buoyancy that, if crossed, could switch circulation into an equilibrium state without strong NADW formation (*7*, *8*). The current consensus is that we are far from any such stability thresholds and that the modern style of vigorous NADW ventilation is a robust feature of warm interglacial climates. Only modest millennial-scale NADW variability has been found to occur during interglacials (*9*, *10*) relative to that seen during colder glacial periods (*11*). However, large but shorter-lived transient anomalies might be possible even in the midst of a generally vigorous interglacial circulation (*7*, *12*, *13*). Hence, reconstructions with appropriate resolution to characterize the short-term instability of NADW during warmer climates are needed to assess model fidelity and constrain possible tipping points for ocean circulation. We used deep sea sediment proxy records from key locations (Fig. 1) to assess the occurrence and magnitude of centennial-scale variability in NADW over the warm interval of the last interglacial period (LIG) [marine isotope stage (MIS) 5e]. The LIG is a useful period for evaluating the sensitivity of NADW to key features that we may face in the future, including a warmer and fresher North Atlantic than at present (*14*, *15*) and the retreat of the circum–North Atlantic cryosphere (*15*, *16*).

We characterized the short-term variability of NADW over the LIG using sediment core MD03-2664 (57°26.34′N, 48°36.35′W; 3442 m water depth) from the Eirik Drift site used to identify the centennial-scale NADW reduction associated with the climate anomaly 8.2 thousand years before the present (ky B.P.) (*12*). This site monitors the newly formed, integrated Nordic Seas overflows (*12*) that are the primary constituents of lower NADW (*1*). The high sedimentation rate (~35 cm ky^{-1}) at this location allows a multidecadal depiction of lower NADW properties and ventilation across the LIG (~30 years per 1-cm sample), which is approximately an order of magnitude greater than the previous reconstructions used to infer millennial-scale NADW stability during the LIG (*10*, *17*).

On our age model (*18*), the MIS 5e "plateau" [the interval of relatively constant minimum ice volume (benthic $\delta^{18}O$)] corresponds to 116.1 to 128.0 ky. We focused our study on this interval, referring to it as the LIG. We documented NADW variability using the carbon isotopic composition

[1]Department of Earth Science, University of Bergen and Bjerknes Centre for Climate Research, Allégaten 41, 5007 Bergen, Norway. [2]Uni Climate, Uni Research and Bjerknes Centre for Climate Research, Bergen, Norway. [3]Institute of Marine and Coastal Sciences and Department of Earth and Planetary Sciences, Rutgers University, New Brunswick, NJ, USA. [4]Laboratorie des Sciences du Climat et de l'Environnement/Institut Pierre Simon Laplace, CEA/CNRS/UVSQ, Gif-sur-Yvette, France. [5]Godwin Laboratory for Paleoclimate Research, Department of Earth Sciences, University of Cambridge, Cambridge, UK.

*Corresponding author. E-mail: eirik.galaasen@geo.uib.no

($\delta^{13}C$) of bottom water, a widely used tracer to delimit the relative influence of low-nutrient (high-$\delta^{13}C$) NADW and nutrient-rich (low-$\delta^{13}C$) Southern Ocean–sourced bottom waters (*19*) (Fig. 1). We reconstructed bottom water $\delta^{13}C$ using the epibenthic foraminifera *Cibicidoides wuellerstorfi*.

Peak epibenthic foraminifera $\delta^{13}C$ values from Eirik Drift core MD03-2664 gradually increased during the LIG by ~0.5 per mil (‰) (Fig. 2), paralleling long-term trends in planktonic and benthic $\delta^{13}C$ records from the Nordic Seas (*20*, *21*) source region for NADW. The similar trends in deep water $\delta^{13}C$ at the Eirik Drift and Nordic Seas indicate a strong influence of Nordic Seas–sourced deep water at the core site during much of the LIG. This suggests that a water mass distribution similar to that of the modern Atlantic, with strong NADW influence, was established after the penultimate deglaciation and persisted on millennial and longer time scales throughout the LIG, as previously observed (*10*, *17*).

Despite this apparent millennial-scale stability, large but short-lived $\delta^{13}C$ decreases indicate that prominent changes in bottom-water chemistry occurred on shorter time scales (Fig. 2). During these multicentennial shifts, epibenthic $\delta^{13}C$ decreased abruptly by up to ~0.7‰, an amplitude similar to that of glacial-interglacial (*19*) and millennial-scale (Dansgaard-Oeschger) changes in the deep Atlantic (*11*). By comparison, the only $\delta^{13}C$ decrease of similar magnitude found at this site during the Holocene occurred after the freshwater outburst from proglacial Lake Agassiz (*12*). Thus, we documented multiple LIG deep water events similar in $\delta^{13}C$ magnitude and duration to that associated with the 8.2 ky B.P. event.

What drove these transient changes in deep Atlantic chemistry? There are indications that similar bottom-water $\delta^{13}C$ reductions occur at deep sites in the subpolar North Atlantic (*22*) and sub-Antarctic Atlantic (*23*) (Fig. 3). This wide geographic distribution (Fig. 1) requires a mechanism able to reduce deep $\delta^{13}C$ at widespread locations and eliminate north-south $\delta^{13}C$ gradients in the abyssal Atlantic. We rule out changes in preformed NADW $\delta^{13}C$ as an explanation because (i) there is no evidence for such $\delta^{13}C$ changes in Nordic Seas source waters during the LIG (*20*, *21*), (ii) the changes are smaller in sites most directly influenced by the Nordic Seas overflows (*22*), and (iii) it would require source water $\delta^{13}C$ changes that were larger and faster than those caused by the recent input of anthropogenic CO_2 (*24*). Instead, the pattern of bottom-water chemical and circulation changes suggests that the Nordic Seas overflows repeatedly decreased in density and/or shoaled to depths shallower than the Eirik Drift during the low-$\delta^{13}C$ excursions. The reduced bottom current vigor observed during the largest $\delta^{13}C$ minimum at ~124 ky B.P. (Fig. 3) is consistent with reduced NADW production (*25*). Sudden incursions of Southern Source Water (SSW) as NADW waned would explain the abrupt (multidecadal) onset of the anomalies as well as the convergence of bottom-water $\delta^{13}C$ toward

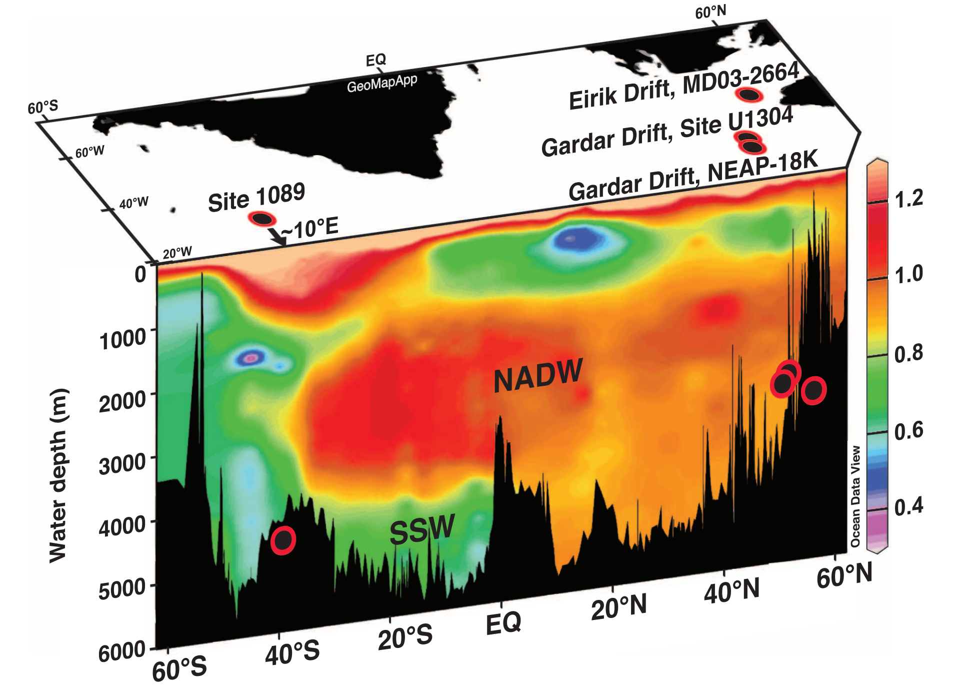

Fig. 1. Locations of core sites. MD03-2664 (57°26′N, 48°36′W; 3442 m), IODP Site U1304 (53°03′N, 33°32′W; 3082 m), NEAP-18K (52°46′N, 30°21′W; 3275 m), and ODP Site 1089 (40°56′S, 9°54′E; 4624 m) (core specifics are summarized in table S1). Core locations are projected onto a north-south section of dissolved inorganic carbon $\delta^{13}C$ (‰) in the Atlantic (World Ocean Circulation Experiment A16) (*36*). High-$\delta^{13}C$ (low-nutrient) NADW occupies the basin at ~2 to 4 km water depth, overlying (high-nutrient) low-$\delta^{13}C$ SSW, corresponding to modern Antarctic Bottom Water.

Fig. 2. Deep-water property changes during the LIG. Plot of epibenthic *C. wuellerstorfi* $\delta^{18}O$ (blue) and $\delta^{13}C$ records (red) with three-point running means (bold lines) from the Eirik Drift (core MD03-2664) versus core depth (bottom) and age (top). VPDB, Vienna Pee Dee belemnite standard. The horizontal gray bar and vertical lines denote the LIG (defined here as the MIS 5e isotopic plateau), and yellow shading denotes LIG periods of pronounced bottom-water $\delta^{13}C$ reductions. Dashed lines indicate intervals with insufficient foraminifera for analysis. *C. wuellerstorfi* $\delta^{13}C$ values of ~0.5‰ (early LIG) to ~1.0‰ (late LIG) are similar to preformed Nordic Seas values (*20*), indicating NADW influence.

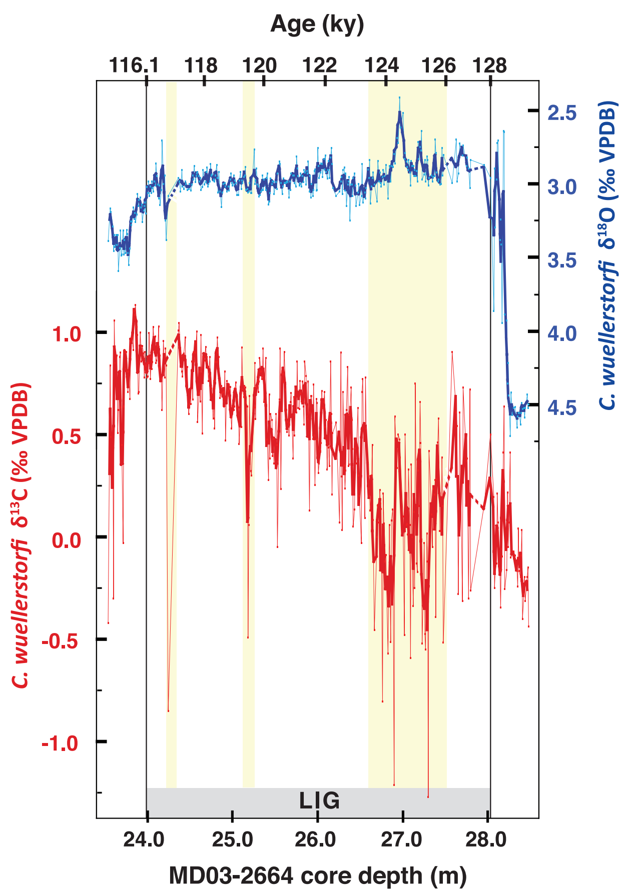

SSW values (≤0.0‰) (*26*) (Fig. 3). Likewise, shoaling and a reduced influx of NADW to the Southern Ocean could explain the decrease in deep circumpolar $\delta^{13}C$ (Fig. 3).

Changes in the production or density of NADW are likely to be linked to changes in North Atlantic source conditions (*7*, *8*). During the LIG, the high northern latitudes were warmer than they are today, and the circum-Arctic marine and terrestrial cryospheres were smaller (*15*, *16*). Models suggest that increased North Atlantic surface buoyancy, due to relative warmth and increased freshwater fluxes from the LIG ice mass retreat, could have inhibited convection and delayed the onset of NADW formation (*14*, *15*). Our results provide an alternative view of deep ocean behavior. Rather than a general suppression of NADW production, our records suggest that relatively brief, intermittent NADW reductions occurred against a background of strong NADW ventilation that was established at the onset of the LIG. This implies a fundamentally different deep ocean behavior, similar to what one might expect from threshold-like flickering of deep convection.

The largest and longest NADW anomalies occur early in the LIG when ice melting was strongest (*15*, *16*, *27*) and residual ice masses from the prior glaciation persisted (*28*). This pattern is reminiscent of the deep ocean and cryosphere coupling apparent in the early Holocene (*12*, *13*). Supporting a connection between ice mass retreat and the NADW reductions, Eirik Drift ice-rafted debris (IRD) deposition and high *Neogloboquadrina pachyderma* (sinistral) Ba/Ca ratios indicate that both iceberg supply and meltwater input persisted during the early LIG (Fig. 4). High Ba/Ca ratios in *N. pachyderma* (s) tests indicate the presence of Ba-rich glacial meltwater inputs (*29*). The increased number of NADW anomalies during the early LIG relative to the Holocene may reflect generally fresher North Atlantic conditions (*14*, *15*), due in part to the greater Greenland Ice Sheet retreat (*16*, *27*). IRD input and Ba/Ca ratios tapered off at the Eirik Drift after ~123.5 and ~124 ky, respectively, suggesting that the stabilization of NADW was coincident with the reduced input of icebergs and glacial meltwater to the North Atlantic (Fig. 4).

Further supporting a role for freshwater forcing in triggering the deep-water anomalies, an outburst flood event analogous to that associated with the 8.2 ky B.P. event occurred during the early LIG (*28*). The detrital layer found throughout the Labrador Sea that is associated with this outburst flood and a marked surface freshening event early in the LIG (*18*, *28*) is also present in our core at ~124.5 ky (*18*) and is followed immediately by the largest and longest NADW reduction of the LIG. This coincidence supports a role for surface buoyancy changes in altering deep Atlantic water mass geometries and bottom-water chemistry. However, it is important to note that the existence of NADW reductions during the second half of the LIG (at ~116.8 and ~119.5 ky; Fig. 3), when conditions favored ice mass expansion rather than rapid retreat (*30*), suggests that decaying ice sheets may not be the sole means of triggering transient NADW reductions. Warming and freshening related to hydrologic changes, as in model simulations of future warming (*5*), could also have increased buoyancy and reduced NADW during the LIG.

The large anomalies in NADW distribution allow us to assess the relationship between climate and deep ocean circulation changes during interglacial periods. Ocean circulation–driven changes in interhemispheric heat transport could explain the inverse long-term Greenland and Antarctic temperature trends over the early LIG (*30*). Likewise, climate was more variable during the LIG than the Holocene (*20, 21*), suggesting a possible link with the increased NADW variability seen in our records. However, evidence for the type of widespread cooling associated with the early Holocene (8.2 ky B.P.) event (*31*) is lacking for the LIG events. This may indicate that sea ice feedbacks, which would be reduced during warmer interglacials, are critical for amplifying the climate response to NADW changes (*32*). Alternatively, it may simply reflect the difficulty of resolving and dating such short-lived LIG events in the proxy records that are currently available. Regardless of the scale of the climate response, Eirik Drift surface proxy reconstructions suggest that a distinct pattern of surface-ocean changes accompanied the NADW reductions. Increases in the abundance of the polar planktonic foraminifera *N. pachyderma* (s) document greater polar water influence in the northwest Atlantic during each NADW reduction (Fig. 4). These polar waters were fresher [marked by lower *N. pachyderma* (s) $\delta^{18}O$] during the early LIG than in the late LIG (Fig. 4), probably reflecting the early high-latitude freshening (*33*). This pattern of southward-displaced polar waters associated with NADW reductions mimics the millennial-scale pattern observed throughout the last glacial cycle (*34*), suggesting that similar ocean-atmosphere dynamics operated during interglacial centennial-scale events. A comparable pattern of changes, though briefer and subtler in character, also marked the Great Salinity Anomaly in the 1960s, when the expansion of fresh polar waters caused cessation of Labrador Sea convection (*35*).

Our results call for a reevaluation of the notion that the deep Atlantic ventilation is relatively stable and vigorous during interglacial periods.

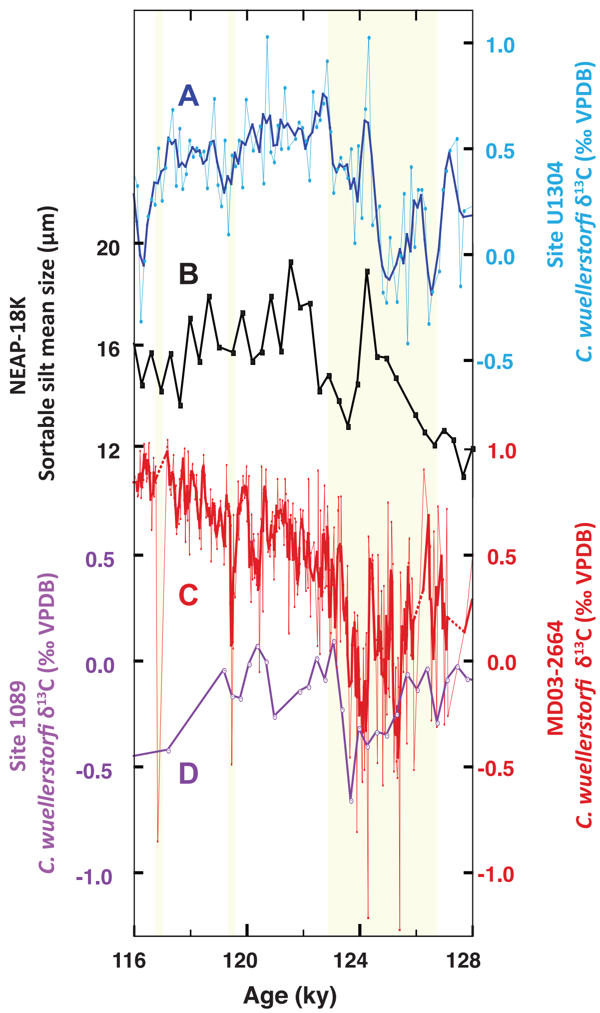

Fig. 3. North and South Atlantic deep-water proxy records spanning the LIG (116.1 to 128.0 ky): *C. wuellerstorfi* $\delta^{13}C$ records from (**A**) IODP Site U1304 with a three-point running mean after (*22*), (**C**) MD03-2664 with a three-point running mean, and (**D**) ODP Site 1089 after (*23*); and (**B**) NEAP-18K sortable silt mean grain sizes after (*25*). Yellow shading marks the interval of high-amplitude variability in all records. Dashed lines in (C) indicate intervals with insufficient foraminifera for analysis.

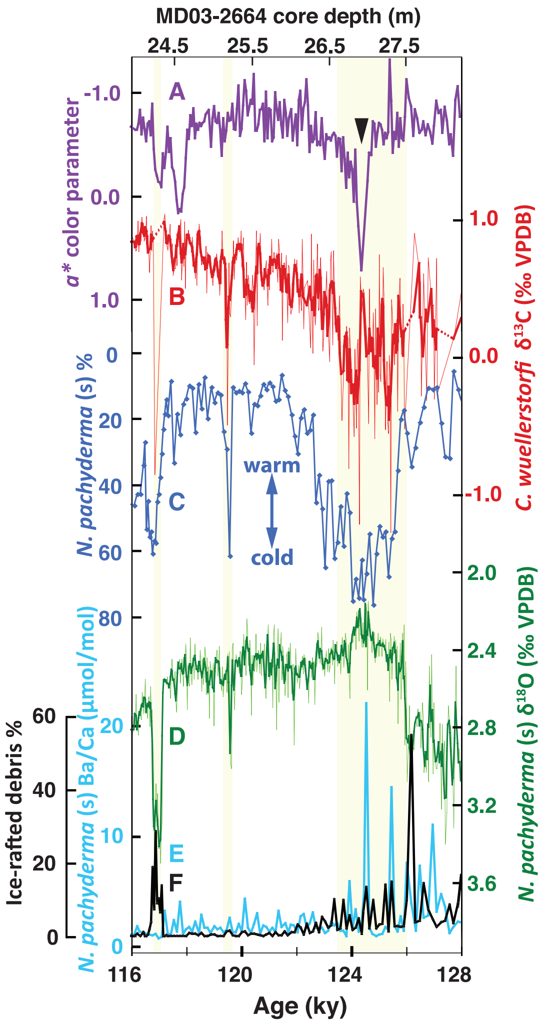

Fig. 4. Proxy records spanning the LIG (116.1 to 128.0 ky) section of core MD03-2664. (**A**) Red-green color parameter a^*, (**B**) *C. wuellerstorfi* $\delta^{13}C$ with a three-point running mean, (**C**) *N. pachyderma* (s) abundance (% of assemblage), (**D**) *N. pachyderma* (s) $\delta^{18}O$ with a three-point running mean, (**E**) *N. pachyderma* (s) Ba/Ca, (μmol/mol), and (**F**) IRD (%) [(C), (D), and (F) are after Irvalı *et al.* (*33*)]. Yellow shading denotes periods of pronounced bottom-water $\delta^{13}C$ reductions. Dashed lines in (B) indicate intervals with insufficient foraminifera *C. wuellerstorfi* for analysis. The triangle in (A) denotes the position of the red detrital layer deposited during an outburst flood event (*18*). The (C) *N. pachyderma* (s) abundance record, a proxy for surface temperature changes in the subpolar North Atlantic region (*14*), indicates changes in Eirik Drift sea surface temperatures.

Our records resolving centennial-scale variability provide clear evidence for large changes in deep Atlantic water mass geometry—similar in magnitude to glacial millennial-scale events—punctuating the LIG. The most prominent NADW reductions occurred during periods of ice sheet melting and known freshwater outbursts, attesting to the importance of surface buoyancy forcing in triggering such events. Concerns about the future evolution of the thermohaline circulation have revolved around the potential existence of inherent tipping points that, if crossed, could lead to long-term perturbations in the mode of ventilation (*7*, *8*), although the existence of such bistability is debated (*6*). The specific characteristics of the observed interglacial NADW anomalies provide insights into the deep ocean's stability and potential impact on a warming world. The shorter duration of the interglacial events as compared to their glacial equivalents indicates that either the forcing or the ocean's inherent response was more transient during warm (interglacial) conditions, arguing against an interglacial deep Atlantic with irreversible tipping points. Nevertheless, the large and rapid variability in deep ocean ventilation also supports the existence of a critical stability threshold; most likely related to deep convection, given the apparent link to surface buoyancy forcing. Although transient in nature, large interglacial anomalies in deep ventilation may still be of particular concern. If triggered, they could alter regional climate (*3*) and CO_2 sequestration pathways (*4*) and in the most extreme cases would as much as double the sea-level increases projected by 2100 CE for densely populated circum–North Atlantic regions (*2*). Our results suggest that past interglacial NADW reductions were abruptly initiated, persisted for centuries, and were concentrated around periods of North Atlantic warmth and freshwater addition, both of which are expected in the future (*5*).

References and Notes

1. R. R. Dickson, J. Brown, *J. Geophys. Res.* **99**, 12319 (1994).
2. A. Levermann, A. Griesel, M. Hofmann, M. Montoya, S. Rahmstorf, *Clim. Dyn.* **24**, 347–354 (2005).
3. T. M. Shanahan *et al.*, *Science* **324**, 377–380 (2009).
4. C. L. Sabine *et al.*, *Science* **305**, 367–371 (2004).
5. IPCC, in *Climate Change 2013: The Physical Science Basis. Contribution of Working Group I to the Fifth Assessment Report of the Intergovernmental Panel on Climate Change*, T. F. Stocker *et al.*, Eds., *Summary for Policymakers* (Cambridge Univ. Press, Cambridge, 2013).
6. M. Hofmann, S. Rahmstorf, *Proc. Natl. Acad. Sci. U.S.A.* **106**, 20584–20589 (2009).
7. T. F. Stocker, A. Schmittner, *Nature* **388**, 862–865 (1997).
8. T. F. Stocker, D. G. Wright, *Nature* **351**, 729–732 (1991).
9. D. W. Oppo, J. F. McManus, J. L. Cullen, *Nature* **422**, 277 (2003).
10. J. F. Adkins, E. A. Boyle, L. Keigwin, E. Cortijo, *Nature* **390**, 154 (1997).
11. L. D. Keigwin, E. A. Boyle, *Paleoceanography* **14**, 164–170 (1999).
12. H. K. F. Kleiven *et al.*, *Science* **319**, 60–64 (2008).
13. C. Kissel, A. Van Toer, C. Laj, E. Cortijo, E. Michel, *Earth Planet. Sci. Lett.* **369-370**, 248–259 (2013).
14. A. Govin *et al.*, *Clim. Past* **8**, 483–507 (2012).
15. B. L. Otto-Bliesner, S. J. Marshall, J. T. Overpeck, G. H. Miller, A. Hu, *Science* **311**, 1751–1753 (2006).
16. E. J. Colville *et al.*, *Science* **333**, 620–623 (2011).
17. D. W. Oppo, M. Horowitz, S. J. Lehman, *Paleoceanography* **12**, 51–63 (1997).
18. See the supplementary materials.
19. W. B. Curry, D. W. Oppo, *Paleoceanography* **20**, PA1017 (2005).
20. T. Fronval, E. Jansen, H. Haflidason, H. P. Sejrup, *Quat. Sci. Rev.* **17**, 963–985 (1998).
21. H. A. Bauch, *Quat. Sci. Rev.* **63**, 1–22 (2013).
22. D. A. Hodell *et al.*, *Earth Planet. Sci. Lett.* **288**, 10–19 (2009).
23. U. S. Ninnemann, C. D. Charles, D. A. Hodell, *Geophys. Monogr. -Am. Geophys. U.* **112**, 99 (1999).
24. A. Olsen, U. Ninnemann, *Science* **330**, 658–659 (2010).
25. I. R. Hall, I. N. McCave, M. R. Chapman, N. J. Shackleton, *Earth Planet. Sci. Lett.* **164**, 15–21 (1998).
26. U. S. Ninnemann, C. D. Charles, *Earth Planet. Sci. Lett.* **201**, 383–396 (2002).
27. A. de Vernal, C. Hillaire-Marcel, *Science* **320**, 1622–1625 (2008).
28. J. A. L. Nicholl *et al.*, *Nat. Geosci.* **5**, 901–904 (2012).
29. J. M. Hall, L.-H. Chan, *Paleoceanography* **19**, PO1017 (2004).
30. NEEM community members, *Nature* **493**, 489–494 (2013).
31. E. J. Rohling, H. Pälike, *Nature* **434**, 975–979 (2005).
32. M. Vellinga, R. A. Wood, *Clim. Change* **54**, 251–267 (2002).
33. N. Irvalı *et al.*, *Paleoceanography* **27**, PA2207 (2012).
34. J. F. McManus *et al.*, *Nature* **371**, 326–329 (1994).
35. R. Dickson, J. Lazier, J. Meincke, P. Rhines, J. Swift, *Prog. Oceanogr.* **38**, 241–295 (1996).
36. R. M. Key *et al.*, *Global Biogeochem. Cycles* **18**, GB4031 (2004).

Acknowledgments: We thank the crew, chief scientist (C. Laj), and scientific party of the R/V *Marion Dufresne*; the Institut Polaire Emile Victorfrom the International Marine Global Changes (IMAGES) P.I.C.A.S.S.O. coring cruise; J. Wright for help locating MIS 5e in MD03-2664; two anonymous reviewers for their insightful and constructive comments; and D. I. Blindheim, O. Hansen, and R. Søraas from the Bjerknes Centre for Climate Research for technical assistance. This study was funded by the Meltzer Fund (University of Bergen) and the North Atlantic Ocean–Climate Variability in a Warmer World (NOCWARM) project (Research Council of Norway) and contributes to EU-FP7 IP Past4Future. The data reported in this paper are tabulated in the supplementary materials.

Supplementary Materials

www.sciencemag.org/content/343/6175/1129/suppl/DC1
Materials and Methods
Supplementary Text
Figs. S1 to S5
Table S1
References (*37*–*54*)
Data Table S1

18 November 2013; accepted 10 February 2014
Published online 20 February 2014;
10.1126/science.1248667